ARL-RR-13 AR-008-383

AD-A284 230

DEPARTMENT OF DEFENCE

DEFENCE SCIENCE AND TECHNOLOGY ORGANISATION

AERONAUTICAL RESEARCH LABORATORY

MELBOURNE, VICTORIA

DISTRIBUTION STATEMENT A
Approved for public release

Research Report 13

RESIDUAL STRENGTH OF COMPOSITES WITH MULTIPLE IMPACT DAMAGE

by

J.J. PAUL
S.C. GALEA
R. JONES

DTIC
ELECTE
SEP 09 1994
S B D

94-29582

DTIC QUALITY INSPECTED 8

Approved for public release.

© COMMONWEALTH OF AUSTRALIA 1994

MARCH 1994

94 9 09 014

This work is copyright. Apart from any use as permitted under the Copyright Act 1968, no part may be reproduced by any process without prior written permission from the Australian Government Publishing Services. Requests and enquiries concerning reproduction and rights should be addressed to the Manager, Commonwealth Information Services, Australian Government Publishing Services, GPO Box 84, Canberra ACT 2601.

THE UNITED STATES NATIONAL TECHNICAL INFORMATION SERVICE IS AUTHORISED TO REPRODUCE AND SELL THIS REPORT

AR-008-383

DEPARTMENT OF DEFENCE
DEFENCE SCIENCE AND TECHNOLOGY ORGANISATION
AERONAUTICAL RESEARCH LABORATORY

Research Report 13

RESIDUAL STRENGTH OF COMPOSITES WITH MULTIPLE IMPACT DAMAGE

by

J.J. PAUL
S.C. GALEA
R. JONES

SUMMARY

In recent years the issue of damage interaction, with particular emphasis on multi-site damage, has been of concern to the aircraft industry. Whilst most attention focused on fuselage lap joints, related problems occur in composite structures which are subjected to multiple impact damage. This paper reveals that, for the cases of multiple impact damage in composite structures investigated, little interaction between damaged regions was observed. Thus a simple repair methodology, previously developed for single impact damaged structures, was applied. This methodology was verified via a coupon test program and an experimental evaluation of two damaged F/A-18 horizontal stabilators.

DSTO AUSTRALIA

DTIC QUALITY INSPECTED 3

© COMMONWEALTH OF AUSTRALIA 1994

POSTAL ADDRESS: **Director, Aeronautical Research Laboratory**
506 Lorimer Street, Fishermens Bend
Victoria 3207, Australia.

TABLE OF CONTENTS

Accession For
NTIS GRA&I ☑
DTIC TAB ☐
Unannounced ☐
Justification
By
Distribution/
Availability Codes
Dist | Avail and/or Special
A-1

1. INTRODUCTION

Graphite/epoxy composites have many advantages for use as structural materials in aircraft, including their formability, high specific strength and stiffness, resistance to cracking by fatigue loading and their immunity to corrosion. However, whilst having these advantages, they are prone to a wide range of defects and damage which may significantly reduce residual strength [1-6]. The problem of low energy impact damage is of particular concern and can cause significant reductions in compressive strength (up to 65% of undamaged strength), [6-12]. Whilst impact can cause a significant amount of delamination, often the only external indication is very slight surface indentation. This type of damage is frequently referred to as "barely visible impact damage" (BVID). Indeed, the problem of BVID is of particular concern because the damage is unlikely to be discovered unless the region is subjected to non-destructive inspection (NDI). However, unfortunately, most routine NDI is unlikely to detect BVID unless potential hot spots are being examined.

In recent years the problem of multiple (impact) damaged sites in close proximity has arisen. In many cases the Structural Repair Manual (SRM) divides the component into zones which can be repaired and zones, which because of their high strains, are classed as irreparable. For multiple impact damage, even if each event lies in a repairable zone, the amount of material required to be removed in order to repair the structure, is often such that the repaired region infringes on the irreparable region and, as a result, renders the structure irreparable.

This problem is somewhat similar to that of multi-site damage (MSD) in fuselage aircraft joints. Here each crack, in isolation, may be acceptable. However, the presence of multiple cracks in close proximity can degrade the residual strength and the damage tolerance of the structure below acceptable levels [13,14]. Indeed, in a series of previous reports [14,15] the authors have presented a detailed understanding of the mechanisms governing the fatigue performance of fuselage lap joints. In this work particular attention was paid to joints containing multi-site damage, and both repaired and unrepaired specimens were tested.

The present paper expands on earlier work undertaken in MSD and shows that, unlike MSD in fuselage joints, there is little damage interaction between multiple impact sites in composites for the cases investigated here. In general there are two possible methods for repairing this type of damage. One approach is to remove the damaged region [16-18] and use an internally scarfed repair. This is very effective, but requires extensive bonding facilities resulting in a significant period of non-utilisation of the component. As previously mentioned, for multiple damage sites, this type of repair often results in the structure being classed as irreparable as the region of scarf extends into the irreparable zones. An alternative approach is to increase the strength by reducing the net sectional stresses [19]. This can be achieved by placing an external patch over the damaged area. For this approach, the simple design methodology presented in [19] is extended to include multiple damage sites and substantiated via a laboratory test program. This methodology was further illustrated by a repair to two damaged horizontal stabilators, which were tested to design limit load [20].

2. MULTIPLE IMPACT DAMAGE

It is highly desirable that procedures are available to account for the possible occurrence of delamination-type defects in the design and certification of composite aircraft structures and in the development of approaches for through-life support, to provide a rationale for repair/reject criteria. This problem was reviewed in [21] where it was shown that for delaminations in:

(a) composite laminates,

(b) step lap joints or

(c) mechanically fastened composite joints,

a stage is reached after which a significant increase in the size of the damage does not significantly reduce the residual strength. This significantly simplifies the methodology for estimating critical damage size. The work of [19] built on this hypothesis to develop a simple formula for the design of externally bonded repairs to impact damaged laminates.

As a result of this work it was found that:

> When the patch material has the same stiffness as the parent laminate the reductions in the T^*[1] and W_{av}[2] energy parameters [19] can be estimated by multiplying the values corresponding to the unrepaired structure with the reduction in the net sectional stress. This infers that the residual strength of a repaired structural component can be estimated by the following simple formula:

$$\frac{\text{Residual Strength(repaired)}}{\text{Residual Strength(unrepaired)}} = \frac{\sigma\text{(unrepaired)}}{\sigma\text{(repaired)}} \qquad (1)$$

The problem of material non-linearity was subsequently tackled in [22]. Here it was shown that the failure parameters, T^*, and energy density, W_{av}, calculated using a non-linear analysis coincided with the values calculated from a linear analysis. This contrasts with the situation for metals where the effect of material non-linearity is often accounted for using the Dugdale analogy. Here the crack length "a" is increased by a plasticity correction factor "a_p" with a subsequent increase in the fracture parameters. For impact damaged laminates the independence of the fracture parameters with respect to material non-linearity again underlines the basic nature of the "failure" mechanisms:

> That as the size of the damage increases a stage is reached after which a significant increase in damage size does not significantly decrease the residual strength.

This infers that, for multiple impact damage sites, as the sites get closer they may, in the limit, behave as one large damage site and, as a result, should not dramatically reduce the residual strength. If this was true then the increase in the residual strength obtained through the application of an externally bonded doubler should also satisfy equation (1). To evaluate this hypothesis a series of laboratory tests were performed.

---

[1] T^* refers to the energy release rate calculated around the crack tip.
[2] W_{av} is the average energy density

2.1 Specimen Fabrication

To evaluate the effect of multiple damage sites and to confirm this hypothesis a series of impact damage tests were performed. The graphite epoxy material used throughout these tests was AS4/3501-6 with a ply configuration of $[(+45_2/-45_2/0_4)_3/90]_S$. Before the specimens were cut from these panels, they were C-scanned to determine the void content of the material. Three cases were considered, viz.:

1) A single impact of 30 mm diameter and a 6 mm diameter hole in the centre of the specimen, see Figure 1a,
2) Two impacts of 30 mm diameter and one diameter apart, see Figure 1b and
3) Specimens impacted as per 1) and 2) above and subsequently repaired with a 16 ply external doubler.

Each specimen was impacted with a 12 mm (1/2") diameter ball bearing with a mass of 1 kg and from a height of 1.3m. The extent of damage was limited by the use of 20, 30 and 40 mm "windows" clamped around the specimen during the impacting. For the single impact specimens all three diameter "windows" were used to produce damage with diameters ranging from approximately 19.8 mm to 39.7 mm. A 6 mm diameter hole was also drilled through the centre of the damaged region of these specimens. For the multiple impact specimens the size of the damage was maintained at 30 mm in diameter. All specimens were subjected to a C-scan of the impacted area and the damage size was approximated from these scans.

2.2 Repair Fabrication

In order to validate the simple design rule previously postulated, it was required that the effective stiffness and ply configuration of the patch be representative of the parent material. Therefore the material used for the patch was AS4/3501-6 and was 16 plies thick, with a ply configuration of $[0_2/+45\text{-}45/\text{-}45+45/0_2]_S$. The ends of the patch were scarfed to reduce the peel stresses in the adhesive. The length of the patch and distance to the edge of the grips were 190 mm and 60 mm, respectively. The patches were bonded to the parent laminate using the cold setting acrylic adhesive FLEXON 241. This adhesive was chosen for its excellent shear strength, ease of application and because environmental effects were not an issue in this test series.

2.3 Thermoelastic Evaluation

To evaluate the structural significance of this damage and to investigate damage interaction effects a thermoelastic scan of the damaged regions was performed. The theory describing the coupling between the mechanical and thermal energy of an elastic body was first published in 1855 by Lord Kelvin [23]. For an elastic isotropic body undergoing cyclic loading this theory states that under adiabatic conditions

$$\Delta T/T_o = K\Delta\sigma_{ii} \qquad (2)$$

where ΔT is the local cyclic change in temperature, T_o is the local absolute temperature, K is the thermoelastic constant, and $\Delta\sigma_{ii}$ is the sum of the cyclic stress amplitude. In [24] this formulation was extended to composite materials and allowance made for the effect of

moisture and various non-linearities. In this case for adiabatic conditions equation (2) takes the form

$$\Delta T/T_o = 1/(\rho C_v)[\partial C_{ijkl}/\partial T \varepsilon_{kl} - \beta_{kl}]\, \Delta \varepsilon_{ij} \qquad (3)$$

where C_{ijkl} is the elasticity tensor, and $\beta_{ij} = \alpha_{kl} C_{ijkl}$ where α_{kl} are the coefficients of thermal expansion. In this context the work presented in [25,26] has shown that impact damage produces large changes in the surface temperature profiles. In contrast to most traditional "passive" methods of non-destructive testing, which merely provide information on the size and location of damage, thermal emission techniques reflect the interaction of the load, geometry and material with the damage, thus highlighting its structural significance.

In the present investigation the thermal emission distributions were measured by a system marked under the trade name SPATE 8000 which has the potential for a spatial and temperature resolution of 0.25 mm^2 and 0.001 K, respectively. Provided that adiabatic conditions are maintained it is possible to use the SPATE output together with equation (3), to obtain stress information on the region of interest.

For the multiple impact damaged specimens a SPATE scan of the impact face was taken while the ends of the specimen were subjected to a constant amplitude sinusoidal uniaxial load of 0 ± 80 kN, the load direction being parallel to the 0° ply direction. The scan step size used was approximately 0.42 mm, and the loading frequency was 10 Hz. The uncalibrated, but smoothed, SPATE results for $\Delta T/T_o$ are shown in Figure 2. This figure shows two distinct highly stress regions, which correspond to the impact damaged regions, with little interaction between the two damage sites. As a result of this investigation it was postulated that the residual strength of the multiple impact damaged specimens should not differ significantly from that obtained for the single impact damaged specimens. Therefore, the residual strength can be estimated as:

$$\text{Residual Strength (multiple impacts)} \equiv \text{Residual Strength (single impact)} \qquad (4)$$

If, as is indicated by these results, there is little damage interaction then equation (1) can also be used to estimate the residual strength of repaired multiple impact damaged laminates. The validity of this approximation will be examined in Section 2.5.2

2.4 Test Methodology

Unrepaired specimens were tested individually while repaired specimens were tested back-to-back [19]. Four strain gauges were bonded on the unrepaired specimen; two above and two below the damage. Each pair was positioned on the mid-width and on opposite faces in order to determine axial and bending strains. The repaired specimen only had two strain gauges located on the patched side. In each case the gauges were 110 mm from the centre of the specimen. The specimens were loaded in compression and to avoid the problem of global buckling an anti-buckling rig was used [12]. All specimens were loaded in compression until failure at a constant rate of 40 kN/minute.

2.5 Results

2.5.1 Single Impact Specimens

All specimens, except two which exhibited extensive bending, produced load versus strain curves which were essentially linear to failure. Specimens 4 and 5 exhibited extensive bending near, and up, to failure thereby reducing the failure load obtained. The failure strains for each specimen are tabulated in Tables 1 (single impact case) and 2 (multiple impact case). These results show that the failure strains follow the asymptotic nature outlined in [6]. The variation in the failure strains, for a given damage size, reflects variations in specimen geometry as well as variations in the structure of the internal damage due to impact. In all cases, the patches and the adhesive bond failed after the parent laminate.

The failure load of the repaired specimen can also be predicted (see Table 1) using equation (1) and only requires a knowledge of the unrepaired residual strength and the change in net sectional stresses due to patching. The change in the net sectional stress can be calculated directly from the change in net sectional area. This result is believed to substantiate the trends predicted in the previous section and significantly simplifies the repair design philosophy.

2.5.2 Multiple Impact Specimens

The failure load for the unrepaired multiple impact damaged specimens, as shown in Table 2, was within approximately 600$\mu\varepsilon$ of that for the single impact case. The multiple impact specimens exhibiting larger residual compressive strains then the single impact specimens. This unexpected result is probably due to the presence of a 6 mm diameter hole in the single impact specimens which reduces both the effective cross-sectional area of the specimen and the lateral constraint in the damage region. However overall these results confirm the hypothesis postulated in Section 2.3 that there is little interaction between damaged sites and that, as a first approximation, each impact damaged site can be treated separately. Similarly, for the repaired specimens the failure strains were within 700$\mu\varepsilon$ of that for the single impact case. As a result, equation (1) was found to provide a reasonable estimate of the failure strain.

3. DAMAGED ASSESSMENT OF AN F/A-18 HORIZONTAL STABILATOR

3.1 Background

To illustrate how this approach can be applied to composite structures, the repair of two damaged F/A-18 horizontal stabilators was undertaken. In one case the stabilator was part of the Composite Repair Engineering Development Program (CREDP). (CREDP is a joint program between the Canadian Forces (CF), the RAAF and the United States Navy (USN) to evaluate the capability of repairing damaged composite components on the F/A-18.) The second stabilator was part of the International Follow On Structural Fatigue Test Program (IFOSTP).

3.2 The CREDP Stabilator Repair

As part of the CREDP program, the Aeronautical Research Laboratory (ARL) was tasked to develop and analyse a repair for a damaged horizontal stabilator, which was initially classed as unserviceable and irreparable due to two fragment strikes from a tracer rocket.

The F/A-18 horizontal stabilator comprises an aluminium honeycomb sandwich structure with graphite/epoxy skins, with fibres oriented in the 0° and $\pm 45^\circ$ directions. The cross-section of the stabilator is fully symmetric. In the region of the damage the skin is 29 plies thick (3.68 mm), but tapers off to 7 plies (0.89 mm) at the leading edge and has incurred extensive local damage to the composite skin and underlying honeycomb, but neither fragment penetrated to the other side of the stabilator. As shown in Figure 3, the two damaged areas are approximately the same size; however there was a slight difference in the impact angle of the two fragment strikes. The location of the damaged zone and ply orientation can be seen in Figure 4.

3.2.1 Structural Evaluation

In order to evaluate the structural significance of the damage, i.e. if the original design was optimised for impact damage, a test rig capable of applying the design loads was required. Fortunately ARL had previously developed a test rig for a dynamic test on the IFOSTP horizontal stabilator. The stabilator was mounted in the rig by means of the spindle, which is used to connect the stabilator to the aircraft. Hence all bending loads applied to the stabilator are transferred to the rig via the spindle. A lever arm connected to the root of the stabilator transfers all the torque loads to the test rig. Static loads were applied to the structure via three flexible air bags. The design of the test rig is such that it allows these air bags to be mounted above or below the test article, as described in reference [27].

Four strain gauge rosettes were located in a rectangular pattern around the damage zone and in the corresponding location on the undamaged skin, see Figure 4. The gauges in each rosette were aligned in the direction of the 0° and $\pm 45^\circ$ fibres. Two displacement transducers, on the upper and lower surface, were placed halfway between the inboard rosettes (1 and 2), in the 0° fibre direction, as seen in Figure 3. The gauge length of the displacement transducers was 385 mm. The strain gauge rosettes and displacement transducers were positioned so as to evaluate the change in compliance of the structure due to the damage.

Displacement and pressure transducers were required to measure the extension and pressure of each air bag. The force applied by each air bag is a function of these two variables and was determined from a calibration graph. The root bending moment (RBM) was calculated and used as the reference load applied to the structure. Three extra displacement transducers were attached to the stabilator at the tip, leading and trailing edges, to measure tip displacement and torque induced by the applied load.

3.2.2 Test Description

The first stage of the investigation involved the application of a static load by incrementing the air bag pressure in steps of 10 kPa. Here the maximum load applied to the structure was not considered to be critical since the primary objective was a comparison between the strains and the compliance on the top and bottom surfaces of the stabilator. Initially, the

air bags were placed underneath the stabilator, producing tension in the damaged surface skin, and a dummy loading and unloading run was performed to allow the structure to settle. Several loading and unloading runs were made in this configuration with strain gauge and transducer readings being conducted at each increment of pressure. The loading was then repeated with the air bags re-configured above the stabilator producing a compressive load in the damaged surface.

3.2.3 Results and Discussion

The Ultimate Bending Moment (UBM) and the Design Limit Bending Moment (DLBM) for the horizontal stabilator are 120.3 kNm (1065 kip-in) and 80.2 kNm (710 kip-in), respectively [27,28]. The RBM was calculated for each load step and the test achieved 31% (47%) and 26% (39%) of the UBM (DLBM) in tension and compression, respectively.

The strain survey results for one loading cycle are shown in Table 3, for the case when a compressive load was applied to the damaged surface. The results for the case of tensile loads applied to the damaged surface are very similar. All strain values are presented in microstrain. Table 3 shows that there was no structurally significant difference between the strain gauge results, for strains in the 0° fibre direction, on the top (damaged) and the bottom (undamaged) surfaces except for gauge D2 which has a 24% to 27% reduction, depending upon the value of the RBM, due to damage. This may be due to the gauge being shielded by the damage. The compliance readings, tabulated at the bottom of the tables as 'U' for the undamaged surface strain and 'D' for the damage surface strain, show no significant difference between the top and bottom surfaces. This implies that the global compliance has not been affected by the damage and indicates that there is little structural degradation. This was confirmed by a thermal elastic evaluation of the damaged region, see [29].

3.2.4 The Finite Element Model

To understand the mechanisms involved in this problem and to assist in designing a repair a finite element analysis was undertaken. The damage section of the horizontal stabilator was modelled by representing the skin as a two-dimensional membrane with effective laminate properties and the underlying honeycomb as three-dimensional iso-parametric brick elements. The small changes in the compliance and the local strains due to damage, as observed in the previous section, suggest the possibility of using an external doubler to repair the damaged stabilator. In this case the adhesive layer was modelled using three-dimensional iso-parametric brick elements with the doubler represented by two-dimensional membrane elements, with an effective laminate property. Three cases were analysed, the undamaged skin, the damaged but unrepaired skin and the damaged and repaired skin. The damaged, but unrepaired, model contained 520 nodes, 128 elements and 1255 degrees of freedom and the repaired model contained 818 nodes, 256 elements and 1976 degrees of freedom.

The material used for the skin and the doubler was again AS4/3501-6 and the associated laminate properties can be found in Table 4. Young's modulus of the honeycomb and the adhesive was taken to be 2000 MPa and 1800 MPa, respectively, with a Poisson's ratio of 0.35 for both. The doubler was 16 plies (2.032 mm) thick and a pressure of 400 MPa was applied along one edge of the skin.

The accuracy of the finite element model was evaluated by comparing the predicted and measured strains, obtained in [27,28]. For the undamaged stabilator the ultimate design bending moment corresponds to a design limit strain ε_{dls} of approximately 4850 $\mu\varepsilon$, see [27,28]. The corresponding predicted strains at the two trailing edge strain gauges, 1 and 3, were approximately 4950 $\mu\varepsilon$ and 4860 $\mu\varepsilon$, respectively, and the predicted value of strain over the region measured by the LVDT was also close to the measured value. However, because the actual structure tapers off towards the leading edge, the strains in the numerical model closest to the leading edge (gauges 2 and 4) were higher than those achieved in the experiment. Nevertheless it was felt that this model would be useful in predicting the change in strain due to the application of an external doubler.

3.2.5 Reduction in Strain due to an External Doubler

Following the development of the undamaged finite element model, two cases were considered. The first case simulated the damaged, but unrepaired, stabilator and the second case modelled a bonded external doubler. A summary of the predicted strains measured by the LVDT and the strains, in the 0^o fibre direction, at gauges 1-4 are given in Table 5.

The application of the external doubler significantly reduced the strain around the damaged zone leading to an average reduction in strain of 28.5%. The peak adhesive shear stress was less than 25 MPa and was below the endurance level of the thin film adhesive FM73, see [30], indicating that the repair should not debond and should be inherently damage tolerant, see [30]. The stress concentration around the damage was also found to be very localised and was consistent with the experimentally measured thermal emission profile [29], as well as with the experimentally measured values of strain and compliance.

3.2.6 Repair Evaluation

Following the initial tests on the horizontal stabilator the damaged region was repaired using an external doubler which was tailored to matched the stiffness of the stabilator skin. The ply configuration of the repaired laminate was $(+45\text{-}45/0_2/90/\text{-}45+45/0)_S$. The loose fibres around the impact zone were removed and the edges of the damage zone were scarfed. The whole region was then filled with packing adhesive and the repair laminate was then bonded onto this surface using FM73 adhesive.

The test procedure, outlined in section 3.2.2, was then repeated with additional strain gauge rosettes placed on the repair. The location of the repair ranged from 0.610m (24") to 1.092m (43") from the root of the stabilator. The repair successfully withstood both tension and compression loading. In tension, the majority of the region exceeded the DLBM. The measured strain reduction was approximately 28% and was equivalent to the reduction in the nett section stress.

3.3 The IFOSTP Stabilator Repair

The previous test article contained both delamination and penetration damage. To assess the problem of BVID in a high strain region a second stabilator test was required. Fortunately a test article which had previously been used to develop the loading mechanisms for the IFOSTP test program was available. The stabilator was impacted at

two sites on the top surface, thus inducing BVID in the composite skin. At each location the absorbed energy was approximately 12 Joules and the size of the damage was constrained to be approximately 30 mm in diameter. The distance between the two impact damage zones was approximately 30 mm (one diameter, as in the coupon test program). Of the two damage sites, see Figure 5, the one closest to the root was in a zone C which was classed as irreparable by the Structural Repair Manual (SRM). The second impact site was located in zone F. As such the SRM repair for the latter damage would have impinged into zone C thus, according to the SRM, this damage is also classed as irreparable. In zone C the ply configuration was [+45/-45/90/0/+45/0/-45/0/90/0/-45/0/45/0/90/-45/45], 17 plies, and in zone F the ply configuration was [+45/-45/90/0/+45/0/-45/90/-45/0/45/0/90/-45/45], 15 plies, i.e. two 0° plies were dropped.

An externally bonded doubler (patch) of dimensions 260 mm by 160 mm and ten plies thick, with a ply configuration of $[+45/-45/90/0_2]_S$, was used to repair this damage. The doubler was designed to reduce the net section stress by approximately 35% thus reducing the stress at the damage locations to under 3000 με at DLBM.

3.3.1 Thermoelastic Evaluation

To investigate the structural interaction between the two damage sites a thermal emission scan of the region was performed. Two electro-magnetic shakers were attached to the underside of the stabilator, at a position that allowed the fundamental bending mode, at approximately 14 Hz, to be excited. The resultant scan can be seen in Figure 6. As in Section 2.5.2, which dealt with multiple impact damage in coupon test specimens, the two damage zones can be clearly seen as well as the change in the stress due to the ply drop off. However, as was also seen in Sections 2.3 and 2.5.2, this scan also supports the hypothesis, first presented in Section 2.1, that there is little interaction between the damage sites. As a result, as a first approximation, each site may be treated in isolation.

3.3.2 Limit Load Test

As in the previous test three air bags were placed underneath the stabilator, producing compression in the damaged surface skin, and a dummy loading and unloading run was performed to allow the structure to settle. Several loading and unloading runs were made in this configuration with strain gauge and transducer readings being conducted at each increment of pressure. The structure was then loaded, incrementing the air bag pressure in steps of 10 kPa, to DLBM. There was no evidence of failure either at the damage location or in the repair and all strain gauge readings varied linearly with load. In this test the strain in zone C, near the first damage site, was measured as approximately -4000 με in the 0° direction, -2500 με in the 45° direction and -500 με in the -45° direction.

4. CONCLUSION

This paper has presented a repair methodology that can be used as a first approximation for field repairs to damaged composite structures. It has been shown that an externally bonded doubler was able to repair impact damage, even for thick structural components. The use of externally bonded patches has the advantage of being quick and easy to apply. The F/A-18 horizontal stabilator repair also indicated that extensive removal of damaged material, excluding penetration clean up, can be avoided thereby making the repair process particularly simple.

REFERENCES

1. Badaliance R. and Dill H.D., "Damage mechanism and life prediction of graphite-epoxy composites". Damage in Composite Materials, ASTM STP 775, 220-242 (1982).
2. Schutz D., Gerharz J.J., and Alschweig, E., "Fatigue properties of unnotched, notched and jointed specimens of a graphite-epoxy composite". Fatigue of Fibrous Composite Materials, ASTM STP 723, 31-47 (1981).
3. Prakash R., "Significance of defects in the fatigue failure of carbon fibre reinforced plastics". Fibre Sci. Technol. 14, 171-181 (1981).
4. Talreja R., "A conceptual framework for the interpretation of fatigue damage mechanisms in composite materials". J. Compos. Technol. Res. 7, 25-29 (1985).
5. Harris B., "Fatigue and accumulation of damage in reinforced plastics". Composites 8, 214-220 (October 1977).
6. Ramkumar R.L., "Compression fatigue behaviour of composites in the presence of delaminations". Damage in Composite Materials, ASTM STP 775, 184-210 (1982).
7. Jones R., Broughton W, Mousley R.F. and Potter R.T., "Compression failures of damage graphite epoxy laminates". Composite Structures 3, 167-186 (1985).
8. Ramkumar R.L., "Effect of low-velocity impact damage on the fatigue behaviour of graphite-epoxy laminates". Long-term Behaviour of Composites, ASTM STP 813, 116-135 (1983).
9. Rosenfield M.S. and Gause L.W., "Compression fatigue behaviour of graphite-epoxy in the presence of stress raisers". Fatigue of Fibrous Composite Materials, ASTM STP 723, 174-196 (1981).
10. Adsit N.R. and Waszczak J.P., "Effect of near-visual damage on the properties of graphite/epoxy". Composite Materials: Testing and Design (Fifth Conference), ASTM STP 674, 101-117 (1979).
11. Starnes J.H., Rhodes Jr. M.D. and Williams J.G., "Effect of impact damage and holes on the compressive strength of a graphite/epoxy laminate". Nondestructive Evaluation and Flaw Criticality for Composite Materials, ASTM STP 696, 145-171 (1979).
12. Saunders D.S., Clark G., van Blaricum T.J. and Preuss T.E., "Graphite/Epoxy coupon testing programme". Theoretical and Applied Fracture Mechanics 13, 105-124 (1990).
13. Molent L., Bridgford N., Rees D. and Jones R., "Environmental evaluation of repairs to fuselage lap joints". Composite Structures 21, 121-130 (1992).
14. Jones R., Rees D. and Kaye R., "Stress analysis of fuselage lap joints". Invited Paper, Symposium on Structural Integrity of Aging Airplanes, edt by S.N. Atluri et al, Springer Verlag Publishers (March 1992).
15. Jones R., Bridgford N., Wallace G. and Molent L., "Bonded repair of Multi-site damage". Structural Integrity of Aging Aircraft, edt by S.N. Atluri et al, Elsevier Applied Science Publishers, Berlin, 199-212 (1991).

16. Hart-Smith L.J., "The design of repairable advanced composite structures, Douglas Paper 7550". Presented to SAE Aerospace Technology Conf., Long Beach, CA (14-17 October 1985).

17. Kurachi E.A. and Hart-Smith L.J., "Design details for adhesively bonded repairs of fibrous composite structures" Douglas Paper 7637 Presented to 31st National Sample Symposium and Exhibition, Las Vegas, NV (8-10 April 1986).

18. Hart-Smith L.J., "Design and anlaysis of bonded repairs for metal aircraft structures". Bonded Repair of Aircraft Structures, edt by A.A. Baker and R. Jones, Martinus Nijhoff, The Hague, 31-46 (1988).

19. Paul J. and Jones R., "Analysis and repair of impact damaged composites". J. Engineering Fracture Mechanics 41, 1, 127-141 (1992).

20. Paul J., "Fibre composite repairs to thick composite structures". Proceedings International Conference on Aircraft Damage Assessment and Repair, edt by R. Jones and N. J. Miller,Published by The Institution of Engineers Australia, ISBN (BOOK) 85825 537 5, 39-45 (July 1991).

21. Jones R., Paul J., Tay T.E., and Williams J.F., "Assessment of the effect of impact damage in composites: some problems and answers". Composite Structures 10, 51-73 (1988).

22. Tay T.E., Paul J. and Jones R., "Effects of plasticity on several fracture parameters for impact damage and related problems". Composite Structures 18, 2, 109-124 (1991).

23. Thomson W. (Lord Kelvin), "On the thermo-elastic and thermo-magnetic properties of matter". Q. J. Maths 1, 55-77, 1855, reprinted in Phil. Mag. 5 (1878).

24. Jones R., Tay T.E., and Williams J.F. "Thermo-mechanical behaviour of composites". Composite Materials Response: Constitutive Relations and Damage Mechanisms, edt by G.C. Sih, Elsevier Applied Science, 49-61 (1988).

25. Heller M., Williams J.F., Dunn S., and Jones R., "Thermo-mechanical analysis of composite specimens". Composite Structures 11, 309-324 (1988).

26. Jones R., Heller M., Lombardo D., Dunn S., Paul J. and Saunders D., "Damage growth in composites". Composites Structures 12, 291-314 (1989).

27. Paul J., "Evaluation of a damaged F/A-18 horizontal stabilator". Aircraft Structures Technical Memorandum 503, Aeronautical Research Laboratory, Melbourne, Australia (1989).

28. Paul J. and Bridgford N. "Analysis of a damaged F/A-18 horizontal stabilator". Aircraft Structures Technical Memorandum 510, Aeronautical Research Laboratory, Melbourne, Australia (1989).

29. Jones R., Heller M., Sparrow J.G. and Ryall T.G., "A new approach to structural optimisation". Composites Structures 16, 1-32 (1990).

30. Chiu W.K., Rees D., Chalkley P. and Jones R., "Designing for damage tolerant repairs". Aircraft Structures Report 450, Aeronautical Research Laboratory, Melbourne, Australia (August 1992).

Table 1: Results of static compression tests: Single impact case

Specimen number	Damage diameter (mm)	Absorbed energy (J)	Damaged area (mm^2)	Unrepaired (U) Required (R)	Failure load (kN)	Failure strain (με)	Predicted strain (με)
1	19.8	7.59	453	U	-191	-4503	--
2	19.8	7.55	453	U	-214	-4680	--
3	19.8	7.96	453	U	-213	-4826	--
4	19.8	5.60	479	R	-238	-4993*	-6164
5	19.8	8.21	428	R	-238	-4993*	-6164
6	19.8	7.84	448	R	-289	-6699	-6164
7	19.8	7.88	458	R	-289	-6699	-6164
8	30.0	7.46	733	U	-168	-4097	--
9	30.0	6.93	718	U	-192	-4375	--
10	30.0	7.88	665	U	-173	-4305	--
11	30.0	7.54	761	U	-196	-4350	--
12	30.0	7.74	761	U	-197	-4274	--
13	30.0	7.67	761	U	-178	-4025	--
14	30.0	7.66	800	R	-233	-5293	-5594
15	30.0	7.35	800	R	-233	-5293	-5594
16	30.0	7.45	739	R	-227	-5554	-5594
17	30.0	7.64	704	R	-227	-5554	-5594
18	39.7	6.25	1252	U	-178	-4061	--
19	39.7	5.76	1252	U	-204	-4445	--
20	39.7	5.87	1252	U	-181	-4090	--
21	39.7	7.83	1385	R	-238	-5337	-5542
22	39.7	7.58	1212	R	-238	-5337	-5542
23	39.7	7.70	1290	R	-222	-5099	-5542
24	39.7	7.59	1120	R	-333	-5099	-5542

* Specimens exhibited extensive bending prior to failure (anti-buckling rig was distorted)

Table 2: Results of static compression tests: Multiple impact case

Specimen number	Impactor diameter (mm)	Absorbed energy site 1 (J)	Absorbed energy site 2 (J)	Unrepaired (U) Required (R)	Failure load (kN)	Failure strain (με)	Predicted strain (με)
25	30.0	8.2	8.4	U	-219	-4861	--
26	30.0	8.72	8.32	U	-211	-4785	--
27	30.0	8.40	8.41	U	-198	-4826	--
28	30.0	8.65	8.32	R	-255	-5954	-6025
29	30.0	8.45	8.57	R	-255	-6024	-6025
30	30.0	8.39	8.55	R	-254	-5773	-6025
31	30.0	8.35	8.33	R	-254	-6264	-6025

Table 3: Strain gauge results for the damaged and undamaged skins on the CREDP horizontal stabilator: Compression case (all measurements in με)

RBM (kNm)		0	-9	-18	-25	-31	-25	-18	-9	0
Torque (kNm)		0	-6	-13	-18	-22	-18	-13	-6	0
Gauge D1	+45	-1	-131	-258	-361	-453	-369	-269	-144	-1
Gauge D1	0	-1	-263	-516	-717	-899	-732	-531	-283	-1
Gauge D1	-45	0	-49	-95	-132	-164	-132	-96	-51	-1
Gauge D2	+45	-1	-64	-125	-175	-219	-176	-127	69	-1
Gauge D2	0	0	-119	-232	-321	-400	-327	-240	-129	-1
Gauge D2	-45	-1	-12	-24	-32	-39	-33	-30	-17	-1
Gauge D3	+45	0	-182	-356	-496	-622	-505	-366	-194	-1
Gauge D3	0	-	423	-827	-1151	-1437	-1156	-831	-434	-2
Gauge D3	-45	0	-95	-186	-259	-325	-262	-191	-101	-2
Gauge D4	+45	-1	-126	-246	-344	-431	-351	-256	-138	-1
Gauge D4	0	-1	-261	-508	-705	-878	-717	-522	-281	-1
Gauge D4	-45	-1	-25	-47	-63	-78	-645	-48	-27	-1
Gauge U1	+45	0	119	232	322	401	328	238	127	-1
Gauge U1	0	-1	260	507	705	877	714	518	275	-1
Gauge U1	-45	0	60	119	165	204	164	118	60	-1
Gauge U2	+45	-1	113	219	304	376	308	224	119	-1
Gauge U2	0	-1	161	316	440	550	446	320	168	-1
Gauge U2	-45	-1	-16	-27	-36	-42	-39	-37	-24	-1
Gauge U3	+45	-1	171	333	463	573	467	339	180	-1
Gauge U3	0	-1	405	790	1097	1357	1107	804	429	-1
Gauge U3	-45	-1	112	218	302	373	304	220	117	-1
Gauge U4	+45	-1	93	182	252	311	252	181	95	-1
Gauge U4	0	-1	257	502	702	872	708	513	272	0
Gauge U4	-45	0	-3	-6	-8	-10	-8	-6	-3	0
U		1	370	734	1038	1285	1067	788	438	0
D		0	-363	-719	-1016	-1260	-1041	-754	-403	0

Table 4: Laminate properties for the horizontal stabilator skin and repair doubler

	E_{XX} (GPa)	E_{YY} (GPa)	G_{XY} (GPa)	ν_{XY}	ν_{YX}
Skin	66.7	32.5	14.5	0.389	0.190
Repair	57.4	32.9	17.2	0.443	0.253

Table 5: Summary of strain results from finite element analysis at DLBM

Strain gauge no.	Unrepaired με	Repaired με	% Reduction
1	4,953	3,557	28
2	4,621	3,399	26
3	5,210	3,658	30
4	4,863	3,522	28
LVDT	5,284	3,664	31

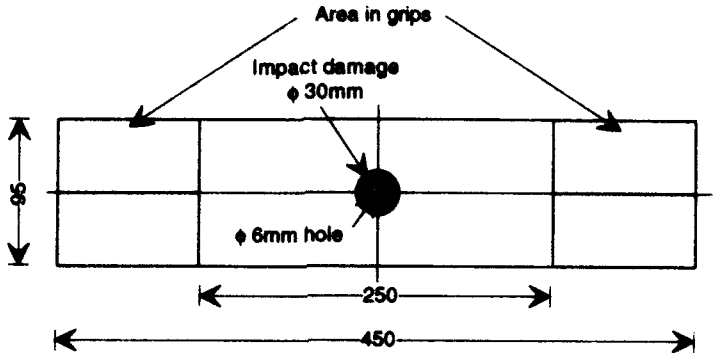

Figure 1a: Single impact specimen configuration.

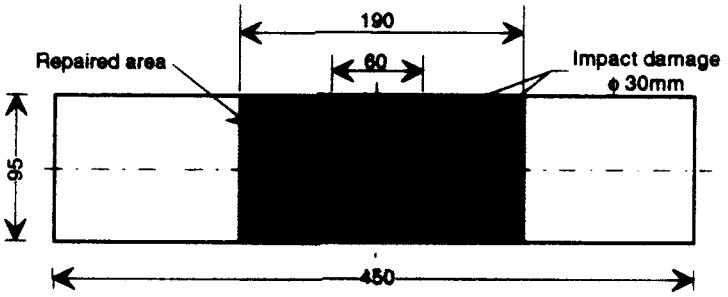

Figure 1b: Multiple impact specimen configuration.

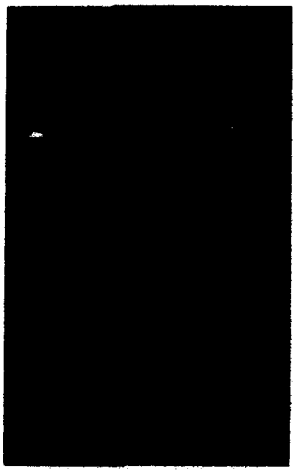

Figure 2: Thermoelastic SPATE output of the multiple impact region on the multiple impact specimen.

Figure 3: Damage zone on the CREDP F/A-18 horizontal stabilator.

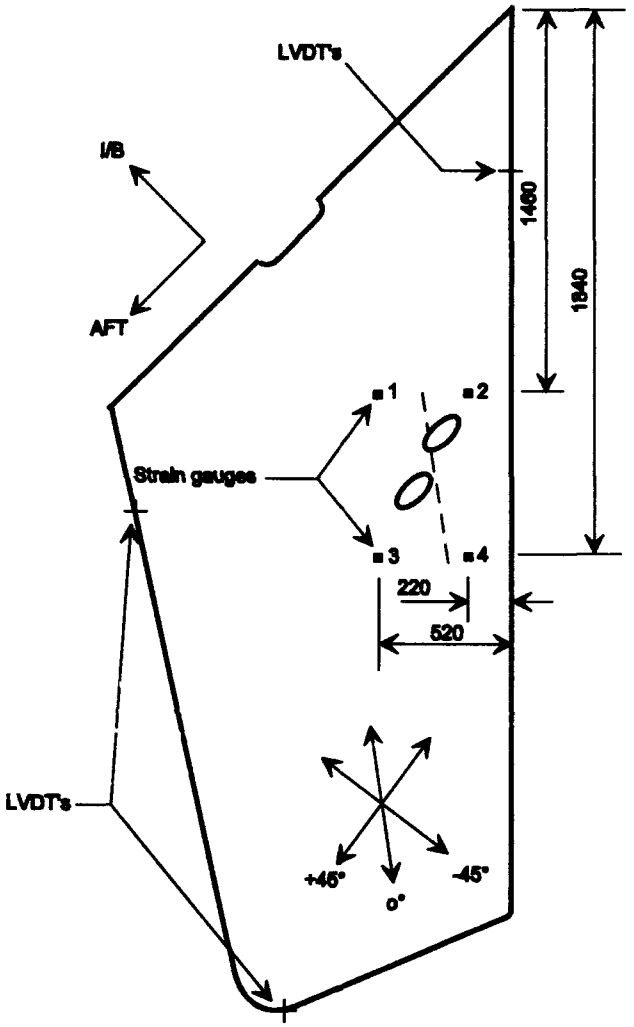

Figure 4: Location of impact damage, strain gauges and displacement transducers on the CREDP F/A-18 horizontal stabilator.

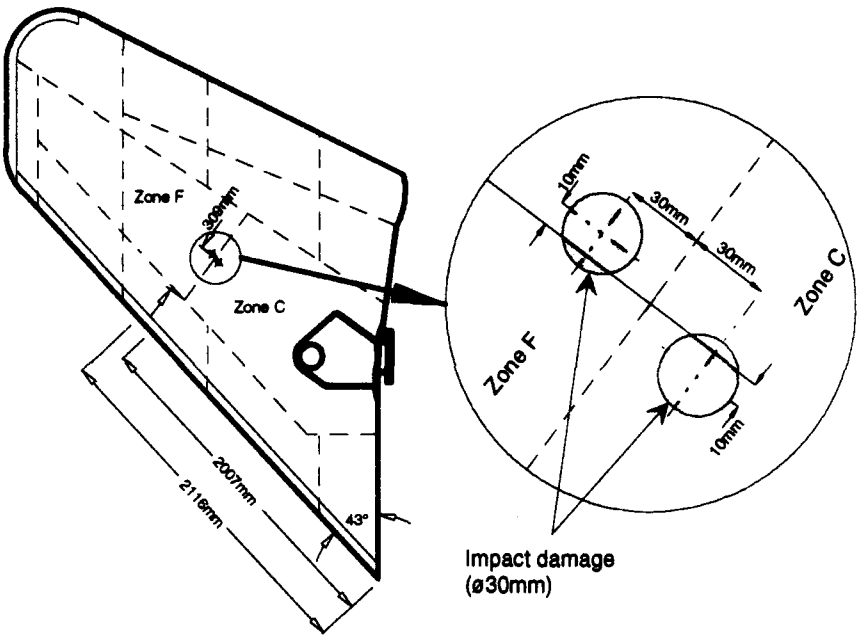

Figure 5: Location of impact damage on the IFOSTP F/A-18 horizontal stabilator.

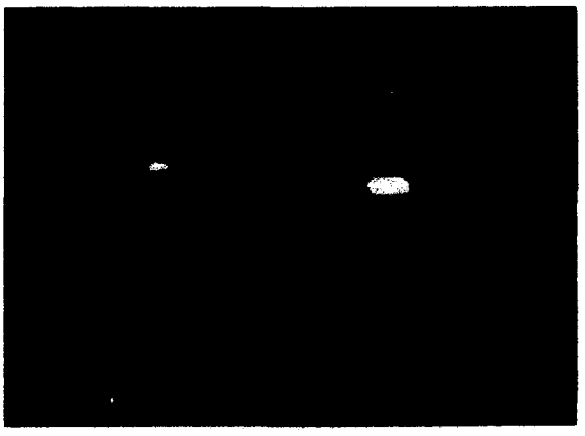

Figure 6: Thermoelastic SPATE output of the multiple impact region on the IFOSTP F/A-18 horizontal stabilator.

DISTRIBUTION

AUSTRALIA

DEFENCE ORGANISATION

Defence Science and Technology Organisation

Chief Defence Scientist
FAS Science Policy
AS Science Corporate Management
} shared copy

Counsellor Defence Science, London (Doc Data Sheet only)
Counsellor Defence Science, Washington (Doc Data Sheet only)
Senior Defence Scientific Adviser (Doc Data Sheet only)
Scientific Advisor Policy and Command (Doc Data Sheet only)
Navy Scientific Adviser (3 copies Doc Data Sheet only)
Scientific Adviser - Army (Doc Data Sheet only)
Air Force Scientific Adviser (Doc Data Sheet only)
Scientific Adviser to Thailand MRD (Doc Data sheet only)
Scientific Adviser to the DRC (Kuala Lumpur) (Doc Data sheet only)

Aeronautical and Maritime Research Laboratory
Director
Library Fishermens Bend
Library Maribyrnong
Chief Airframes and Engines Division
Author(s): R. Jones
J. Paul
S. Galea (3 copies)
R. Chester
A. Baker
F. Rose
R. Callinan

Main Library - DSTO Salisbury

Defence Central

OIC TRS, Defence Central Library
Document Exchange Centre, DSTIC (8 copies)
Defence Intelligence Organisation
Library, Defence Signals Directorate (Doc Data Sheet Only)

HQ ADF

Director General Force Development (Air)

Navy

Director of Aircraft Engineering - Navy
Director of Naval Architecture

Army

Engineering Development Establishment Library
US Army Research, Development and Standardisation Group (3 copies)

Air Force

PDR AF
DENGPP-AF
AHQ CSPT
CLSA-LC
OIC ATF, ATS, RAAFSTT, WAGGA (2 copies)

UNIVERSITIES AND COLLEGES

Australian Defence Force Academy
Library
Head of Aerospace and Mechanical Engineering

Flinders
Library

LaTrobe
Library

Melbourne
Engineering Library

Monash
Hargrave Library
Head, Materials Engineering

Newcastle
Library
Institute of Aviation

New England
Library

Sydney
Engineering Library
Head, School of Civil Engineering

NSW
Physical Sciences Library
Head, Mechanical Engineering
Head, Fuel Technology

Queensland
Library

Tasmania
Engineering Library

Western Australia
Library
Head, Mechanical Engineering

RMIT
Library
Aerospace Engineering

University College of the Northern Territory
Library

OTHER GOVERNMENT DEPARTMENTS AND AGENCIES

AGPS
Department of Transport & Communication, Library
Civil Aviation Authority
Australian Nuclear Science and Technology Organisation

OTHER ORGANISATIONS

NASA (Canberra)
ASTA Engineering, Document Control Office
Ansett Airlines of Australia, Library
Qantas Airways Limited
Hawker de Havilland Aust Pty Ltd, Victoria, Library
Hawker de Havilland Aust Pty Ltd, Bankstown, Library
Rolls Royce of Australia Pty Ltd, Manager

SPARES (7 COPIES)

TOTAL (78 COPIES)

AL 149 DEPARTMENT OF DEFENCE

DOCUMENT CONTROL DATA

PAGE CLASSIFICATION
UNCLASSIFIED

PRIVACY MARKING

1a. AR NUMBER	1b. ESTABLISHMENT NUMBER	2. DOCUMENT DATE	3. TASK NUMBER
AR-008-383	ARL-RR-13	MARCH 1994	AIR 91/056

4. TITLE

RESIDUAL STRENGTH OF COMPOSITES WITH MULTIPLE IMPACT DAMAGE

5. SECURITY CLASSIFICATION (PLACE APPROPRIATE CLASSIFICATION IN BOX(S) IE. SECRET (S), CONF. (C) RESTRICTED (R), LIMITED (L), UNCLASSIFIED (U)).

DOCUMENT	TITLE	ABSTRACT
U	U	U

6. NO. PAGES: 20

7. NO. REFS.: 30

8. AUTHOR(S)

J.J. PAUL
S.C. GALEA
R. JONES

9. DOWNGRADING/DELIMITING INSTRUCTIONS

Not applicable.

10. CORPORATE AUTHOR AND ADDRESS

AERONAUTICAL RESEARCH LABORATORY

AIRFRAMES AND ENGINES DIVISION

506 LORIMER STREET

FISHERMENS BEND VIC 3207

11. OFFICE/POSITION RESPONSIBLE FOR:

SPONSOR: RAAF DTA

SECURITY: -

DOWNGRADING: -

APPROVAL: CAED

12. SECONDARY DISTRIBUTION (OF THIS DOCUMENT)

Approved for public release.

OVERSEAS ENQUIRIES OUTSIDE STATED LIMITATIONS SHOULD BE REFERRED THROUGH DSTIC, ADMINISTRATIVE SERVICES BRANCH, DEPARTMENT OF DEFENCE, ANZAC PARK WEST OFFICES, ACT 2601

13a. THIS DOCUMENT MAY BE ANNOUNCED IN CATALOGUES AND AWARENESS SERVICES AVAILABLE TO ....

No limitations

14. DESCRIPTORS

Damage assessment	F/A-18 aircraft
Composite structures	Stabilators
Impact damage	Evaluation
Repair	

15. DISCAT SUBJECT CATEGORIES: 0103

16. ABSTRACT

In recent years the issue of damage interaction, with particular emphasis on multi-site damage, has been of concern to the aircraft industry. Whilst most attention focused on fuselage lap joints, related problems occur in composite structures which are subjected to multiple impac damage. This paper reveals that, for the cases of multiple impact damage in composite structures investigated, little interaction between damaged regions was observed. Thus a simple repair methodology, previously developed for single impact damaged structures, was applied. This methodology was verified via a coupon test program and an experimental evaluation of two damaged F/A-18 horizontal stabilators.

PAGE CLASSIFICATION
UNCLASSIFIED
PRIVACY MARKING

THIS PAGE IS TO BE USED TO RECORD INFORMATION WHICH IS REQUIRED BY THE ESTABLISHMENT FOR ITS OWN USE BUT WHICH WILL NOT BE ADDED TO THE DISTB DATA UNLESS SPECIFICALLY REQUESTED.

16. ABSTRACT (CONT).

17. IMPRINT

AERONAUTICAL RESEARCH LABORATORY, MELBOURNE

18. DOCUMENT SERIES AND NUMBER	19. WA NUMBER	20. TYPE OF REPORT AND PERIOD COVERED
Research Report 13	21 218F	

21. COMPUTER PROGRAMS USED

22. ESTABLISHMENT FILE REF.(S)

23. ADDITIONAL INFORMATION (AS REQUIRED)